GEOPHYSICS, VOL. 63, NO. 5 (SEPTEMBER-OCTOBER 1998); P. 1629–1647, 19 FIGS., 1 TABLE.

3-D symmetric sampling

Gijs J. O. Vermeer*

ABSTRACT

Three-dimensional seismic surveys have become accepted in the industry as a means of acquiring detailed information on the subsurface. Yet, the cost of 3-D seismic data acquisition is and will always be considerable, making it highly important to select the right 3-D acquisition geometry. Up till now, no really comprehensive theory existed to tell what constitutes a good 3-D geometry and how such a geometry can be designed. The theory of 3-D symmetric sampling proposed in this paper is intended to fill this gap and may serve as a sound basis for 3-D geometry design and analysis.

Methods and theories for the design of 2-D surveys were developed in the 1980s. Anstey proposed the stack-array approach, Ongkiehong and Askin the hands-off acquisition technique, and Vermeer introduced symmetric sampling theory. In this paper, the theory of symmetric sampling for 2-D geometries is expanded to the most important 3-D geometries currently in use. Essential elements in 3-D symmetric sampling are the spatial properties of a geometry. Spatial aspects are important because most seismic processing programs operate in some spatial domain by combining neighboring traces into new output traces, and because it is the spatial behavior of the 3-D seismic volume that the interpreter has to translate into maps.

Over time, various survey geometries have been devised for the acquisition of 3-D seismic data. All geometries constitute some compromise with respect to full sampling of the 5-D prestack wavefield (four spatial coordinates describing shot and receiver position, and traveltime as fifth coordinate). It turns out that most geometries can be considered as a collection of 3-D subsets of the 5-D wavefield, each subset having only two varying spatial coordinates. The spatial attributes of the traces in each subset vary slowly and regularly, and this property provides spatial continuity to the 3-D survey. The spatial continuity can be exploited optimally if the subsets are properly sampled and if their extent is maximized.

The 2-D symmetric sampling criteria—equal shot and receiver intervals, and equal shot and receiver patterns—apply also to 3-D symmetric sampling but have to be supplemented with additional criteria that are different for different geometries. The additional criterion for orthogonal geometry (geometry with parallel shotlines orthogonal to parallel receiver lines) is to ensure that the maximum cross-line offset is equal to the maximum in-line offset.

Three-dimensional symmetric sampling simplifies the design of 3-D acquisition geometries. A simple checklist of geophysical requirements (spatial continuity, resolution, mappability of shallow and deep objectives, and signal-to-noise ratio) limits the choice of survey parameters. In these considerations, offset and azimuth distributions are implicitly being taken care of.

The implementation in the field requires careful planning to prevent loss of spatial continuity.

INTRODUCTION

Since the early 1980s, there has been a steady increase in the number of 3-D surveys acquired each year. Continuing improvements in technology have made it possible to make 3-D seismic data acquisition more and more efficient and cost-effective. Yet, a clear theory as to what constitutes a good 3-D acquisition geometry has not been available, and much of the design of 3-D acquisition geometries has been based on earlier experience—what seemed to have worked in the past was adopted for the future—and on the possibilities and limitations of the available equipment (Stone, 1994). In this paper, I provide a theoretical framework for the design of 3-D acquisition geometries suitable for both marine and land data acquisition.

Quite rightly, many current design techniques for 3-D geometries attempt to extend to 3-D what had been learned

Manuscript received by the Editor January 14, 1997; revised manuscript received March 16, 1998.
*Formerly Shell International Exploration and Production B.V., Research and Technical Services; presently 3DSymSam—Geophysical Advice, Maduroweg 3, 2252 TS Voorschoten, The Netherlands. Phone: 31-71-561-1516; E-mail: vermeerg@worldonline.nl.

from the design of 2-D geometries. A breakthrough in thinking about 2-D geometries was provided in Anstey's paper (1986) "Whatever happened to ground roll?". Anstey argued that the combination of field arrays and stacking takes care of adequate suppression of ground roll, provided the offset distribution in the common midpoint (CMP) is regular and dense, the so-called stack-array concept. Ongkiehong and Askin (1988) proposed the hands-off seismic data acquisition concept. They argued that the distance between elements in an array and the length of the contiguous arrays is fully determined by signal velocity and required bandwidth. These ideas are encompassed and reexplained by the symmetric sampling theory introduced in Vermeer (1990, 1991). In symmetric sampling, both shots and receivers have to be sampled in the same way, including the shot and receiver arrays. In this theory, a regular offset distribution in the CMP gather is a consequence of the requirement of symmetric sampling.

Anstey's (1986) considerations on offset distributions valid for 2-D could be applied also to 3-D marine streamer acquisition because it is basically 3-D by repeating 2-D. However, these considerations are not applicable generally to land-type acquisition geometries such as the orthogonal arrangement of shot and receiver lines. On the other hand, 2-D symmetric sampling theory can be extended to 3-D for all types of common 3-D geometries. As we shall see, symmetric sampling of the 2-D seismic line is in fact a special case of *3-D symmetric sampling*. At the 1994 SEG annual meeting, I first proposed the 3-D symmetric sampling technique (Vermeer, 1994). The present paper provides a more comprehensive description.

In 2-D, the sampling problem is one of sampling the 3-D wavefield $W(t, x_s, x_r)$ with temporal coordinate t, shot coordinate x_s, and receiver coordinate x_r. In 2-D symmetric sampling, the two spatial (shot and receiver) coordinates are sampled in the same way. Using sufficiently small sampling intervals allows the faithful reconstruction of the underlying continuous wavefield, i.e., it maintains the spatial continuity of the wavefield $W(t, x_s, x_r)$.

In 3-D, we are faced with the sampling of a 5-D wavefield $W(t, x_s, y_s, x_r, y_r)$, now with shot y_s and receiver y_r as additional spatial coordinates. It would be prohibitively expensive to completely sample this 5-D wavefield, as this would mean filling the whole survey area with a dense coverage of both shots and receivers. As a compromise, 3-D symmetric sampling settles for the more affordable aim of correct sampling of overlapping single-fold 3-D subsets of the 5-D wavefield $W(t, x_s, y_s, x_r, y_r)$. Such correctly sampled subsets are suitable for imaging of the subsurface with the right resolution (provided the source wavelet has a suitably wide bandwidth) using prestack migration (Beylkin, 1985; Beylkin et al., 1985; Cohen et al., 1986; Bleistein, 1987; Schleicher et al., 1993). The subsets have to be spatially overlapping (multifold acquisition) to gain redundancy for an adequate signal-to-noise ratio and to allow velocity analysis.

To set the scene, I first show that geometries most commonly used are either members of the class of areal geometries or members of the class of line geometries. The line geometries can be subdivided further into parallel, orthogonal, and zigzag geometries. I then extend some of the results of Vermeer (1990) to a description of some properties of the continuous wavefield and various 3-D subsets of that wavefield. These properties are used to describe the requirements of symmetric sampling of the two spatial coordinates of each subset.

Next, I discuss the link between symmetric sampling and the design of 3-D geometries and how that link should influence the implementation of the design in the presence of obstacles in the field. Though not substantiated with examples, it is plausible that 3-D symmetric sampling can be exploited beneficially in prestack processing. Finally, I show that for low-fold data, the offset distribution should be irregular for the best stack response.

In this paper, I do not discuss multicomponent recording separately, though most results apply without major modification.

CLASSES OF 3-D GEOMETRIES

Alias-free sampling of all four spatial (surface) coordinates of the 5-D prestack wavefield $W(t, x_s, y_s, x_r, y_r)$ would mean that each shot should be recorded by a dense areal grid of receivers and that the shotpoints should also occupy a dense areal grid. Virtually nobody can afford this full sampling of $W(t, x_s, y_s, x_r, y_r)$. Instead, a wide variety of geometries has been devised based on a sparser sampling of shots and/or receivers.

Most solutions to the seismic sampling problem can be classified into one of two main classes: (1) the receivers listening to each shot still occupy a dense areal grid, but the shots are sampled in only a coarse grid (or the other way around), and (2) the receivers listening to each shot are densely sampled along one or more parallel receiver lines, whereas the shots are densely sampled along parallel shotlines. The geometries in the first class are called *areal* geometries, whereas those in the second class are called *line* geometries. Depending on the orientation of the shotlines with respect to the receiver lines, the line geometries can be subdivided into three main types: parallel, orthogonal, and zigzag. Figure 1 provides a pictorial description of areal and line geometries. Note that the shotlines in the main types of line geometries are parallel to each other, whereas the receiver lines are also parallel to each other (in zigzag geometry, there are two sets of parallel shotlines making an angle of $\pm 45^\circ$ with the parallel receiver lines).

[In Vermeer (1994), I used the term "patch" for the areal geometry. The term "patch" was adopted from the geometry described in Crews et al. (1989). They use areal patches of geophones listening to a sparse grid of shots. Unfortunately, the term patch is used in the geophysical industry also for particular implementations of line geometries. Therefore, in this paper I have opted for the name "areal" to emphasize the difference with line geometries. Of course, all geometries want to achieve an areal coverage.]

Virtually all geometries can be classified as areal or line geometries. *Random* geometries are characterized by the absence of regularity in the shot and receiver positions.

Examples of various geometries

Areal geometry provides either 3-D common-shot gathers (as defined by an areal grid of receivers listening to a shot in the center of the grid) or 3-D common-receiver gathers. The idea to acquire 3-D common-shot gathers with a 2-D array of receivers was patented as early as 1960 (Becker, 1960). Walton (1971) called the 3-D common-shot gather "The dream." Part of his dream was to hover with a helicopter over the area on a dark night and watch the geophones light up when a sound wave hit them. [A modern version of this idea using laser interferometry is described in Berni (1994).] It turned out to be more practical to invoke reciprocity and to use an areal grid

of thumper positions being recorded in a geophone patch in the center. Esso (now Exxon) used this technique in several surveys (Walton, 1971), but abandoned it in favor of the more cost-effective "X" spread technique.

The technology in the 1970s was not yet advanced enough to allow multiple-coverage areal geometries. This changed in the 1980s, and Crews et al. (1989) contains an acquisition technique that is reminiscent of multiple-coverage areal geometry. However, instead of a full areal grid, each shot is recorded by a checkerboard pattern of geophone stations. It would require double the effort to acquire a true areal geometry. On land, this is kind of a tall order, as obstructions usually abound.

With the advent of stationary recording systems in marine data acquisition, it is becoming feasible (though still quite time-consuming) to record 3-D common-receiver gathers with receiver stations located on the sea bottom (or anchored to the sea bottom) and with shots fired in a dense areal grid. A geometry coming close to the ideal areal geometry is described in Moldoveanu et al. (1994). They used a dual-hydrophone Digiseis system for undershooting of platforms. An interesting aspect of this geometry is that z_r, the depth coordinate of the receiver, is sampled twice.

[In the introduction, I omitted the depth coordinate from the prestack wavefield because this coordinate is not a variable being sampled in surface seismic data acquisition. (Of course, in VSP acquisition, depth is a major spatial coordinate.) An areal geometry in which z_r is sampled up to 16 times is described in Stubblefield (1990) and in Krail (1991, 1993).]

Depending on the conditions in the survey area, one of the various line geometries is usually the most efficient in terms of progress per square kilometer, and this might be the decisive factor in choosing the type of line geometry. It goes without saying that the most efficient geometry does not necessarily produce the best quality.

Parallel geometry is basically an extension of 2-D geometry where the shot lines and receiver lines are collinear. It is used mainly for marine data acquisition, using multisource and multistreamer configurations (e.g., quad/quad geometry; Naylor, 1990), but it has also been used on land (e.g., Dickinson et al., 1990). In quad/quad geometry, four sources are alternately fired into four streamers. Each source records its own four midpoint lines, leading to 16 parallel midpoint lines. As the seismic vessel has to maintain speed during the firing cycle, the distance between shots in a midpoint line must be large, leading to relatively low fold. This shortcoming has been solved by recent developments in marine acquisition technology, allowing towing of 8–12 streamers by one vessel. With two sources, modern seismic vessels can also produce 16 or more midpoint lines in one boat pass, while doubling the fold as compared to using four sources.

An interesting example of marine data acquisition using parallel acquisition lines is (concentric) circle shoot geometry (Durrani et al., 1987; Reilly, 1995). In this geometry, shot and receiver lines are (nearly) concentric circles. It is a typical example of a target-oriented geometry, the center of all circular lines being the known position of a salt dome.

In parallel geometry, the survey area is still covered rather densely with shots and receivers. In the 1960s, it was already discovered that an orthogonal arrangement of a shot line and a receiver line could produce areal midpoint coverage without requiring an areal coverage of shots and receivers (Ball and Mounce, 1967). In the late 1960s, Esso acquired single-fold 3-D surveys consisting of single "X" spreads or cross-spreads (Walton, 1971, 1972). Properties of the cross-spread and interpretation techniques based on timeslices through cross-spreads are discussed in Dunkin and Levin (1971). In those days, the single-fold cross-spreads were still a big burden to the interpreter but, with the advent of digital processing, the data from partially overlapping cross-spreads could be stacked and migrated for easier interpretation (Dürschner, 1984). Recently, Lee et al. (1994) discussed migration results of partially overlapping cross-spreads.

The idea of areal midpoint coverage by orthogonal shot and receiver lines is fully exploited in orthogonal geometry. In this geometry, widely spaced parallel shotlines are perpendicular to widely spaced parallel receiver lines (see Figure 1).

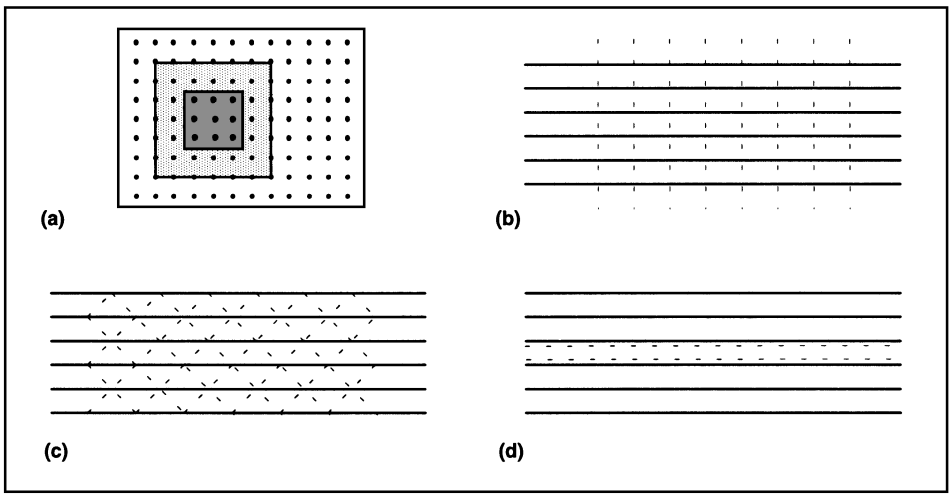

FIG. 1. Classes of 3-D acquisition geometries: (a) areal, (b) orthogonal, (c) zigzag, and (d) parallel. Areal geometry is based on widely spaced shot stations covered areally by receiver stations (or the other way around). The small square and the large square respectively indicate the midpoint area and the receiver area for a shot in the center of the squares. Orthogonal geometry is characterized by widely spaced parallel shot lines perpendicular to widely spaced parallel receiver lines. In zigzag geometry, two families of widely spaced parallel shot lines make angles of $\pm 45^\circ$ with widely spaced parallel receiver lines. In parallel geometry, both shot and receiver lines are parallel with each other; the lines may or may not be widely spaced.

This is a typical land geometry, allowing 3-D coverage with a minimum of field effort. There are numerous variations on this theme, with brick-wall geometry and cross-spread geometry (Dickinson et al., 1990) as the two main implementations. In brick-wall geometry, staggered shotlines are used; in cross-spread geometry, the shotlines are sampled more or less regularly. Orthogonal geometry may also be used for marine data acquisition using ocean-bottom cables.

Zigzag geometry is another land geometry, but now the shots are fired along zigzag lines between the receiver lines. Zigzags between adjacent pairs of receiver lines are arranged such that two sets of parallel shotlines are obtained eventually (see Figure 1). The zigzag geometry is very efficient for data acquisition in deserts (Onderwaater et al., 1996; Wams and Rozemond, 1997).

[Apart from the three main types of line geometries, the seisloop method (Ritchie, 1991)—an early attempt at cost-effective 3-D land acquisition—may also be mentioned. In this geometry areal midpoint coverage is reached by distributing shots and receivers along a closed loop of (curved) lines as, for instance, provided by a road system.]

An example of random geometry is described in Bertelli et al. (1993), where it is applied in an area surrounding the city of Milan, Italy.

THE CONTINUOUS WAVEFIELD

In the literature dealing with migration and inversion (e.g., Beylkin et al., 1985; Cohen et al., 1986; Schleicher et al., 1993), it is often tacitly assumed that the seismic wavefield is a continuous function of its temporal and spatial variables. The assumption of continuity, of course, is justified for the wavefield generated by a single source (apart from near-field discontinuities in case of dynamite as a source). The justification of the assumption of continuity as a function of source coordinates is based on an idealized world in which there are no source wavelet variations. In the following, I also assume that $W(t, x_s, y_s, x_r, y_r)$ can be considered as a continuous function of its variables.

This section deals with the properties of this continuous wavefield to establish requirements for proper sampling. In the acquisition of seismic data, the 5-D wavefield $W(t, x_s, y_s, x_r, y_r)$ is sampled at individual source and receiver locations. The assumption of continuity means that small shifts in source or receiver position would lead to only small changes in the wavefield. Proper sampling of the continuous wavefield allows full reconstruction of that wavefield.

The shot/receiver and midpoint/offset coordinate systems

As in the 2-D case discussed in Vermeer (1990), we can express the wavefield not only in the shot and receiver coordinates, but also in the midpoint and offset coordinates. It is often convenient to use half-offset rather than offset. The midpoint and half-offset coordinates (x_m, h) can be expressed in the shot/receiver coordinates (x_s, x_r):

$$\mathbf{x}_m = (\mathbf{x}_r + \mathbf{x}_s)/2$$
$$\mathbf{h} = (\mathbf{x}_r - \mathbf{x}_s)/2 \qquad (1)$$

in which vector notation is used for each coordinate pair. The orientation of $\mathbf{h}(h_x, h_y)$ describes the shot/receiver azimuth, whereas h_x and h_y describe what are also called in-line offset and cross-line offset, respectively.

The reciprocity theorem

In the description of the properties of the 5-D wavefield $W(t, x_s, y_s, x_r, y_r)$, the reciprocity theorem plays an important role. The theorem says that, under certain conditions (see, e.g., Vermeer, 1990), two seismic experiments in which the position of shot and receiver are interchanged lead to the same recorded trace. A consequence of the reciprocity theorem is that a 3-D common-shot gather $W(t, x, y, x_r, y_r)$ shot at point (x, y) would consist of the same data as a 3-D common-receiver gather $W(t, x_s, y_s, x, y)$ recorded in the same point (x, y). Therefore, the properties of the wavefield in the common-receiver gather, consisting of a large number of different seismic experiments, are the same as the properties of the wavefield of the common-shot gather obtained in a single seismic experiment.

3-D subsets of 5-D wavefield

It is interesting to consider various 3-D subsets (cross-sections) of the 5-D prestack wavefield. In these subsets, we keep the temporal coordinate, together with two spatial coordinates. For instance, in case the two varying spatial coordinates are x_r and y_r, then the subset corresponds to a single shot. It turns out that (except for random geometry) each of the acquisition geometries introduced in "Classes of 3-D geometries" has its own subsets. I call these subsets *basic subsets* of the geometry. Table 1 lists them. Note that in the column with "Description", it is assumed implicitly that each subset is a continuous function of its variables. X and Y are fixed points. Figure 2 illustrates how the various subsets can be generated in the field, keeping two coordinates fixed, while allowing two other coordinates to vary.

The areal geometries can be thought of as either a collection of single-fold 3-D common-shot gathers or single-fold 3-D common-receiver gathers. For the time being, we assume a continuous areal coverage of receivers for the geometry with widely spaced shots and, similarly, a continuous areal coverage of shots for the geometry with widely spaced receivers.

Considering each shot line and each receiver line in the line geometries as a continuous coverage of shots and receivers along those lines leads naturally to the basic subsets of the line geometries. A basic subset is formed by all traces that have a shot line and a receiver line in common. For orthogonal geometry, the basic subset is called the cross-spread (also

Table 1. Basic subsets of various 3-D geometries in 5-D prestack wavefield.

Geometry	Basic subset	Description
Areal	3-D common shot	$W(t, X, Y, x_r, y_r)$
	3-D common receiver	$W(t, x_s, y_s, X, Y)$
Orthogonal	Cross-spread	$W(t, X, y_s, x_r, Y)$
Zigzag	Zig spread	$W(t, x_s, x_s + Y - X, x_r, Y)$
	Zag spread	$W(t, x_s, -x_s + Y + X, x_r, Y)$
Parallel	Midpoint line	$W(t, x_s, Y, x_r, Y)$
	Common-offset gather	$W(t, x_s, y_s, x_s + X, y_s)$

for brick-wall geometry, see next section). In zigzag geometry, we have zig- and zag-spreads (because of the two orthogonal families of shot lines), and in parallel geometry the combination of a shot line and a receiver line is just the midpoint line. In the ideal parallel geometry, the common-offset gather with constant azimuth is another 3-D subset. Figure 3 schematically illustrates the subsets of the line geometries.

All basic subsets are also single-fold, except the midpoint line. The midpoint line does not provide areal coverage, whereas the other subsets do. The number of overlapping single-fold subsets at any point determines the fold-of-coverage in that point (see also the Appendix).

Because each subset is generated in its own specific way, each subset will see the same subsurface structure in a different way. This is illustrated in Figure 4 for a diffractor and for a dipping plane in a constant-velocity medium. The traveltime contours are shown for a 3-D common-shot gather, a cross-spread, a zig-spread, and for a common-offset gather with constant azimuth. The contours are displayed as a function of the xy coordinates of the midpoints. The traveltime surfaces in Figure 4a are all versions of Cheops pyramid (Claerbout, 1985), but each one is computed in a different 3-D subspace of the 5-D space containing our prestack wavefield. Figure 4 illustrates that each subset represents a spatially continuous domain in the 5-D prestack wavefield.

The *c*ommon-*o*ffset gather with constant shot/receiver azimuth (COA gather) covers the whole survey area, whereas the other subsets have a limited extent. The COA gather is therefore better suited for prestack migration than any of the other subsets. As we shall see, however, it is virtually impossible to acquire COA gathers at a reasonable cost. A disadvantage of COA gathers is the single shooting direction. Some subsurface structures can best be illuminated using a wide range of azimuths (cf. O'Connell et al., 1993; Reilly, 1995).

All single-fold subsets mentioned in Table 1 lend themselves to true-amplitude 3-D prestack migration. In fact, various authors dealing with prestack migration implicitly or explicitly assume a 3-D single-fold subset and derive formulas for the migration of such data sets (Beylkin et al., 1985; Cohen et al., 1986; Schleicher et al., 1993; Vermeer, 1995). The subsets are also suitable for imaging with dip moveout (DMO) (Vermeer et al., 1995; Pleshkevitch, 1996; Padhi and Holley, 1997). Padhi and Holley (1997) named those single-fold subsets "minimal data sets" (i.e., data sets minimally required for imaging). This general suitability for imaging of the various basic subsets suggests that their sampling must get due attention.

But before discussing sampling, it is helpful to first discuss the subsets of orthogonal geometry and zigzag geometry in some more detail.

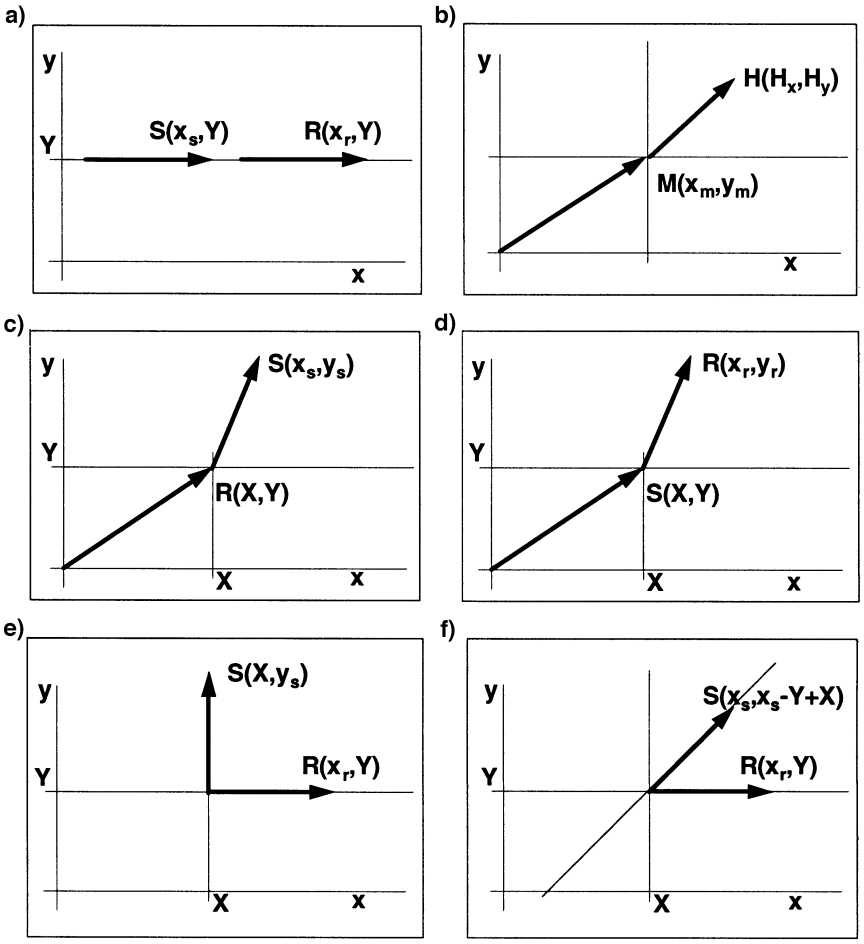

FIG. 2. Various ways of generating 3-D subsets of the 5-D prestack wavefield: (a) 2-D line, (b) common-offset gather with constant shot/receiver azimuth, (c) 3-D receiver gather, (d) 3-D shot gather, (e) cross-spread, (f) zig spread. X, Y are fixed, whereas lower case coordinates vary in the subset; S is shot, R is receiver.

The cross-spread

Orthogonal geometry consists of more or less straight acquisition lines which may be widely spaced. In the field, the data are acquired in swaths, which may consist of a series of shots (sometimes called a shot salvo) shooting center-spread into the active receivers of an even number of receiver lines (see bottom part of Figure 5). Other swath implementations are also in use. Cross-spreads can be extracted from the orthogonal geometry by collecting all traces that have a shot line and a receiver line in common. Hence, there are as many cross-spreads as there are intersections between shot lines and receiver lines.

Figure 5 highlights the shots and receivers corresponding to one cross-spread in an orthogonal 3-D survey. The midpoint area of the cross-spread is indicated for a wide as well as for a narrow geometry. The maximum in-line offset of this geometry is given by the distance of the farthest active receiver from the shot line, and the maximum cross-line offset is given by the distance of the farthest shot from the receiver line. The ratio of these two distances (cross-line/in-line) determines the aspect ratio of the cross-spread, which is the same as the aspect ratio of the swath.

Figure 6 illustrates some of the properties of the cross-spread. The trace at midpoint M is a member of a common-shot gather, a common-receiver gather, a common-offset gather, and a common-azimuth gather. The midpoints of the common-offset gather form a circle; therefore, horizontal layers show up as circles in the timeslices of a cross-spread (Figure 7). The midpoints of a common-azimuth gather lie along a straight line through the origin of the cross-spread.

Each trace in the 3-D survey is an element of a unique cross-spread. The neighbors of the trace in the cross-spread have

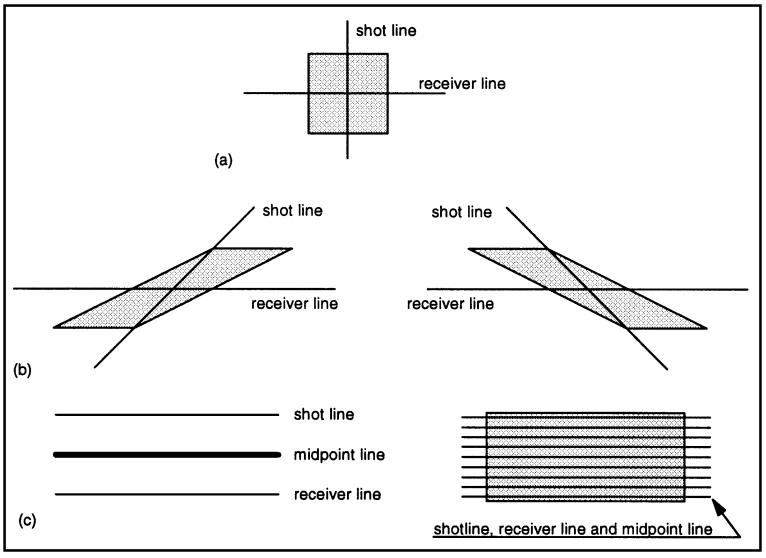

FIG. 3. Basic subsets of line geometries: (a) orthogonal, (b) zigzag, and (c) parallel. Shaded areas indicate the midpoint areas of the subsets. The basic subset of orthogonal geometry is the cross-spread. Zigzag geometry can be decomposed into subsets consisting of zig- and zag-spreads. Parallel geometry has two possible basic subsets: the midpoint line (left) or the common-offset common-azimuth gather (right). The latter may be acquired using repeated 2-D surveys.

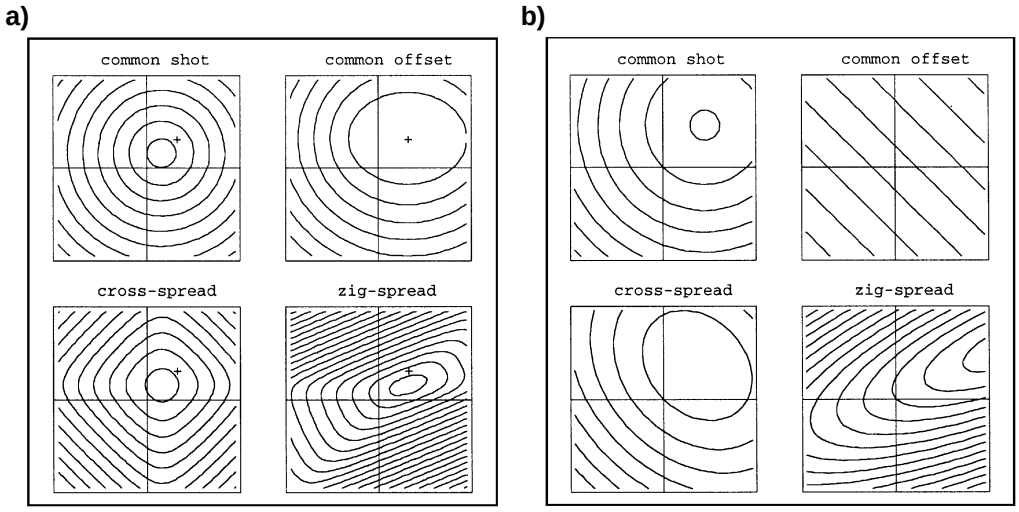

FIG. 4. Traveltime contours in 3-D subsets for the case of a diffraction (a) and a dipping plane (b). The contours are displayed as a function of the (x, y)-coordinates of the midpoints. The position of the diffractor at (500,500,500) is indicated by the "+" symbol.

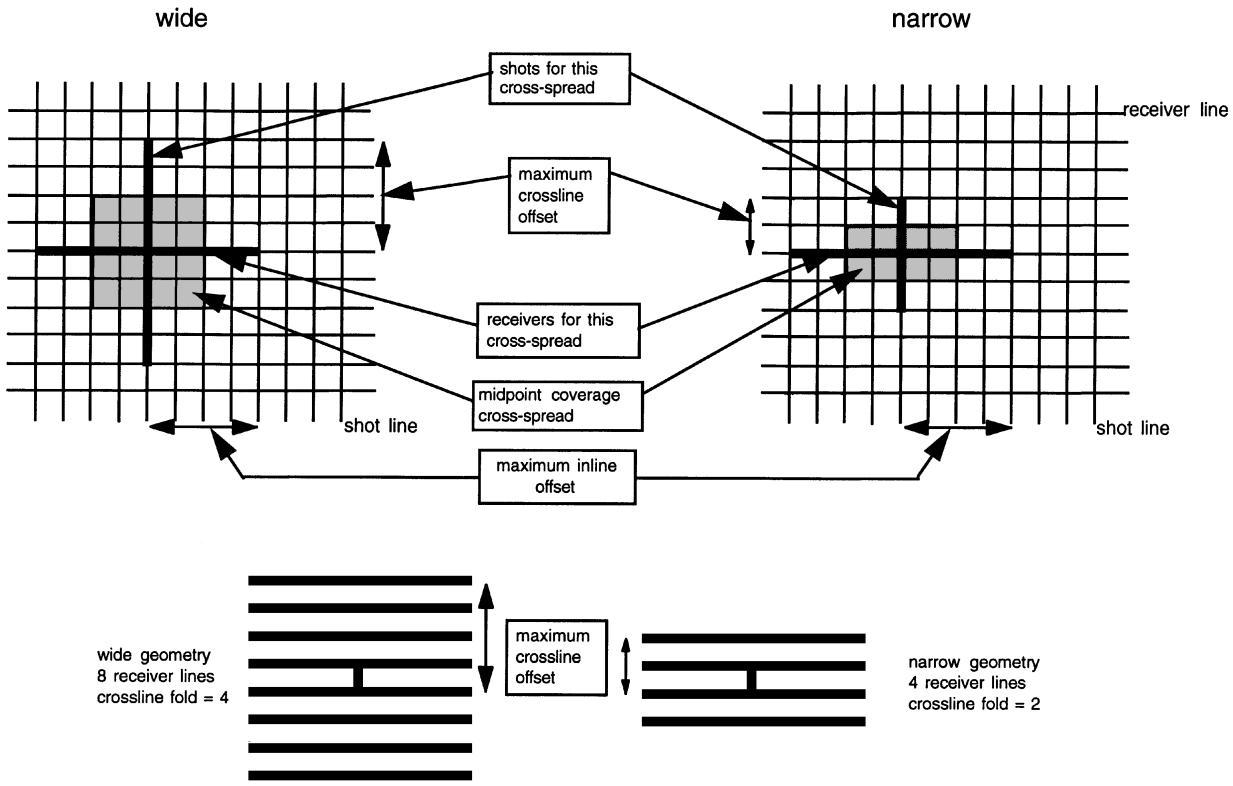

FIG. 5. Cross-spread as subset of a wide orthogonal geometry and a narrow orthogonal geometry. Vertical lines are shotlines; horizontal lines are receiver lines. The bottom part of the figure shows the generating swaths with a series of shots (the shot salvo) in the middle. After these shots have been acquired, the swath moves up to acquire the next shot salvo. The maximum cross-line offset depends on the number of receiver lines and determines whether a wide or a narrow geometry is acquired.

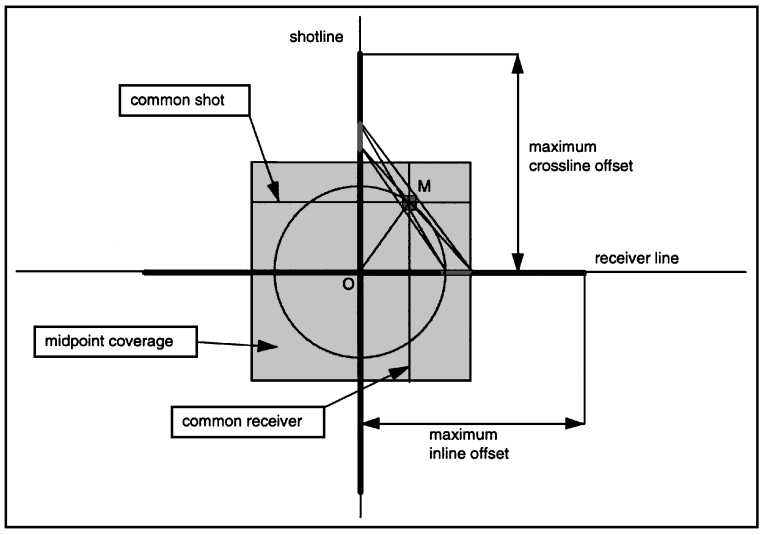

FIG. 6. Properties of cross-spread. The half-offset of a trace at M equals the distance to the center O of the cross-spread (i.e., traces with same offset lie on a circle). The trace is both part of a common-shot gather (horizontal through M) and part of a common-receiver gather (vertical through M). All traces close to M correspond to neighboring shots on the shot line and to neighboring receivers on the receiver line.

been shot by the same or by adjacent shots, and have been recorded by the same or by adjacent receivers. In other words, the spatial attributes of the traces around M vary slowly, making the cross-spread a spatially continuous data set. On the other hand, the maximum useful offset limits the extent of each cross-spread (in a time-variant way), and the edges of the cross-spreads form spatial discontinuities in orthogonal geometry.

If staggered shotlines are used (as in brick-wall geometry), the shot lines are only partially sampled, leading to cross-spreads that are split into a number of strips. The number of edges in this geometry is much larger than in the continuous shot-line geometry; spatial continuity in this geometry is therefore degraded.

Subsets of zigzag geometry

In the field, zigzag geometry is acquired by zigzagging (at 45° angles with the receiver lines) with the sources between two adjacent receiver lines. A swath may consist of four or more receiver lines listening to each shot. The maximum cross-line offset is equal to $n/2+1$ receiver line intervals, where n is the number of active receiver lines. Figure 8 shows how the pattern of source trajectories can be arranged such that all zig parts form continuous lines across the receiver lines, whereas the zag parts form another set of straight shot lines. In this arrangement, zig-spreads as well as zag-spreads can be gathered from the recorded data. The maximum cross-line offset in the zig- and zag-spreads is equal to the maximum cross-line offset in the swath.

Normally, each shot is recorded center-spread, which means that the active receivers move with each shot. As a consequence, the number of traces in a common-receiver gather (in a zig- or zag-spread) is not constant, but the number of traces in a common–in-line–offset gather is. Current practice is to move the shots in the in-line direction over a distance equal to the receiver station interval. This leads to a shot interval that is the square root of two times the receiver interval. In this geometry, the acquired offsets are the same as in an orthogonal geometry with the same spread length and the same number of receiver lines, but the offset distribution is different.

Figure 9 illustrates some properties of the zig-spread. Any trace in this spread is a member of a common-shot gather, a common-receiver gather (parallel to the shot line), a common–in-line-offset gather (parallel to the edges of the zig-spread), a common-offset gather, and a common-azimuth gather. Note

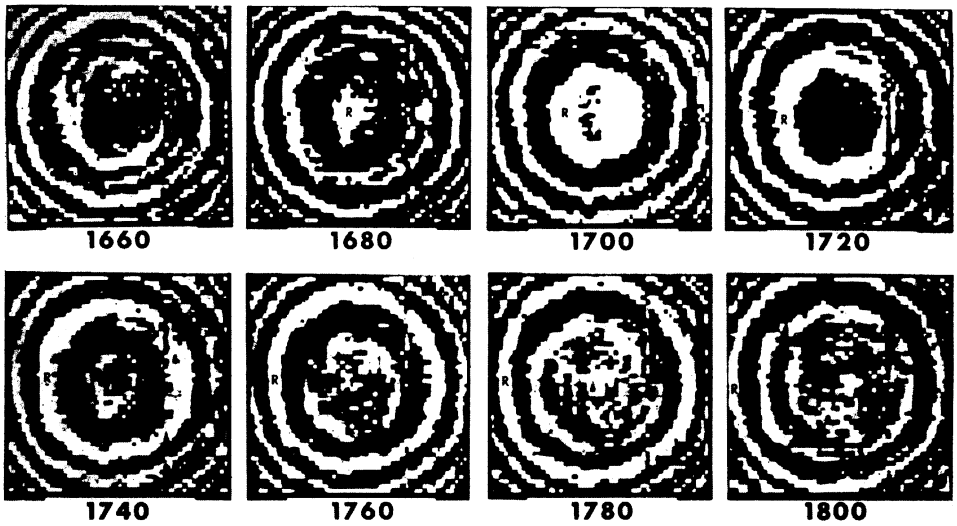

FIG. 7. Timeslices through cross-spread. Taken from Walton (1972).

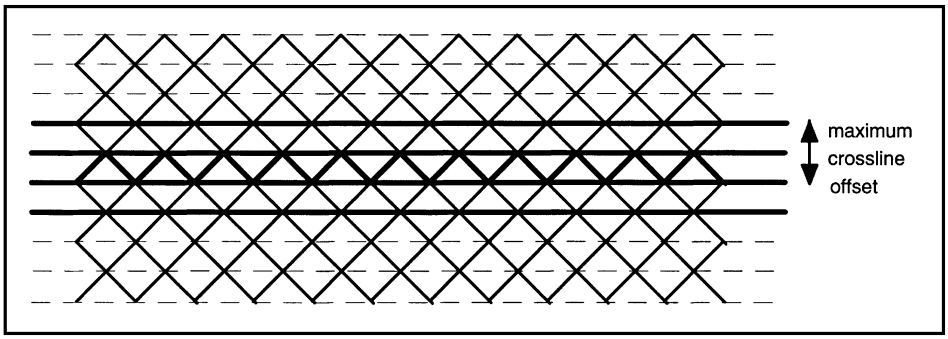

FIG. 8. Zigzag geometry. Vibrators zigzag between two adjacent receiver lines, while (in this case) four spreads of receivers record each shot. A zig-spread can be gathered by taking data acquired with adjacent swaths. Four zig segments make up the shot line in the zig-spread.

that the midpoints of the common-offset gather now form an ellipse. If the maximum cross-line offset equals the maximum in-line offset, the corresponding offset ellipse touches all four edges of the diamond-shaped zig-spread.

A special case of the zigzag geometry is the double zigzag (Onderwaater et al., 1996; Wams and Rozemond, 1997). In this geometry, two zigzags (both with the same zigzag period) are traversed instead of one. The second zigzag is separated from the first zigzag by one quarter of the zigzag period to produce an optimal offset distribution (in a four-line geometry with line spacing four times station interval). The advantage of this geometry is the much better stack response as compared to the single zigzag geometry (cf. Figure 19).

2-D SYMMETRIC SAMPLING

Symmetric sampling was first introduced for 2-D lines in my book *Seismic wavefield sampling* (Vermeer, 1990). Although it is a bit dicey to try and summarize a whole book within half a page, I'll try to list here the most relevant points of 2-D symmetric sampling. Full details can be found in Vermeer (1990).

1) Because of reciprocity, the properties of the continuous wavefield in the common-shot gather are the same as the properties in the common-receiver gather. Therefore, sampling requirements are the same in both domains, leading to symmetric sampling.
2) a. The basic sampling interval Δx is defined as the sampling interval required for alias-free spatial sampling of the whole continuous wavefield (including ground roll, or other low-velocity noise):

$$\Delta x = \frac{1}{2k_{max}} = \frac{V_{min}}{2f_{max}}, \qquad (2)$$

where k_{max} is the maximum wavenumber, V_{min} is minimum apparent velocity, and f_{max} is maximum frequency, all measured in the common-shot gather (or in the common-receiver gather).

b. The basic signal sampling interval d is defined as the sampling interval required for alias-free spatial sampling of the desired part of the continuous wavefield (normally P-wave energy, excluding ground roll or other low-velocity noise). The interval d is governed by the same formula as Δx, but now V_{min} is the minimum recorded apparent velocity in the desired part of the wavefield.
3) The basic sampling interval may be much smaller than anybody is willing to pay for. For example, for a ground-roll velocity of 300 m/s and maximum frequency (in the ground roll) of 60 Hz, a spatial sampling interval of 2.5 m would be required. An alternative is to sample the wavefield with the basic signal sampling interval, and to use shot and receiver arrays as anti-alias filters and resampling operators. Receiver arrays serve as anti-alias filters in the common-shot domain, and shot arrays serve as anti-alias filters in the common-receiver domain. To preserve symmetry, shot and receiver arrays should have equal length and have an equal number of elements.
4) Choosing the number of elements N in a linear array as $N = d/\Delta x$, adjacent (nonoverlapping) arrays are formed which still sample the wavefield at the basic sampling interval Δx and resample it to the basic signal sampling interval d. The array response of this array is

$$a(k) = \frac{\sin(N\pi k\Delta x)}{N\sin(\pi k\Delta x)} = \frac{\sin(\pi kd)}{N\sin(\pi k\Delta x)}, \qquad (3)$$

where k is the wavenumber (inverse of wavelength) in the corresponding shot or receiver domain. The passband of this filter is $-1/d < k < 1/d$. At $|k| = 1/d$, the response is zero, and the suppression band is at $|k| > 1/d$. For a sampling interval d, the Nyquist wavenumber is at $k = \pm 1/(2d)$. To achieve a suppression band for $|k| > 1/(2d)$, a running mix of two arrays can be applied in the processing center.
5) Because the array response has strong side lobes in the suppression band, the anti-aliasing effect of a linear array is far from optimal.
6) Low-velocity noise coming in from the sides (e.g., side scatterers) will have large apparent velocity along the (linear) array. This noise will fall in the passband of the array, but can be suppressed if an areal array is used.

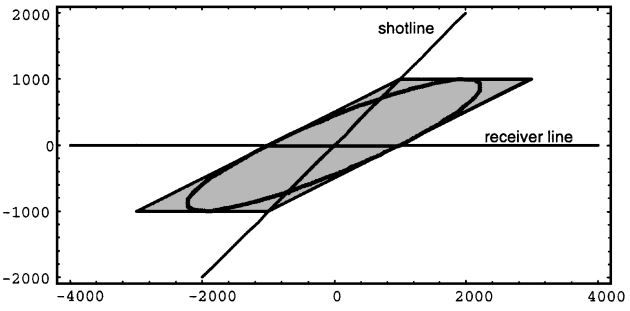

FIG. 9. Zig-spread with equal maximum in-line and maximum cross-line offsets. Note that the receiver spread moves with the shot, ensuring center-spread acquisition for all shots. The rhomboid gray area is the midpoint area of the zig-spread. Horizontal lines represent common shots; oblique lines parallel to the edges of the zig-spread represent common-inline offsets. The ellipse inscribed within the rhomboid represents midpoints with offset equal to the maximum in-line offset.

In the next section, 3-D symmetric sampling is introduced. It turns out that 2-D symmetric sampling is just a special case of 3-D symmetric sampling.

3-D SYMMETRIC SAMPLING

One approach to 3-D survey design (e.g., mega-bin survey technique, Goodway and Ragan, 1997) attempts to sample all four spatial coordinates of the 5-D prestack wavefield as well as possible. Because of the high cost of dense sampling, this objective leads to coarse sampling of the four spatial coordinates with ensuing difficulties in the application of spatial filters and prestack migration. Alias-free sampling of the whole 5-D prestack wavefield is clearly too expensive. Often, it is also impractical, as it requires free access to the whole survey area. Instead, in the 3-D symmetric sampling approach, we attempt to properly sample the single-fold subsets of the chosen areal or line geometry. If we succeed in that more modest objective, the continuous wavefield of the subset underlying the samples can be reconstructed fully. This more modest aim is achieved by dense enough sampling of the varying coordinates in each subset (cf. Figure 2 and Table 1). Usually, sampling of a subset

will provide a single-fold (except in the case of sampling the 2-D line) data set of limited extent. As illustrated in Figure 5 for an orthogonal geometry, partially overlapping subsets need to be sampled to cover the whole survey area.

Of all basic subsets listed in Table 1, only the common-offset gather may extend across the whole survey area. All other single-fold basic subsets have limited areal extent in practice, because offset increases toward the edges in those subsets (cf. Figure 6 for cross-spread) and the target depth has a maximum useful shot/receiver offset. Often the extent of those subsets is maximized in only one spatial direction. A large extent in both spatial directions would fully exploit the potential of each geometry. Therefore, besides alias-free sampling of the basic subsets, we should maximize the (useful) areal extent of the subsets with limited extent. This prescription maximizes the spatial continuity in the 3-D survey and, for a given fold, minimizes the number of edges in the survey.

Together, alias-free sampling of the basic subsets and maximizing the extent of each subset form a generic prescription of 3-D symmetric sampling.

The requirements of 2-D symmetric sampling—equal shot and receiver sampling intervals, and equal shot and receiver arrays—apply without change to the sampling of the subsets of the various 3-D line geometries. However, apart from the 2-D symmetric sampling criteria, each 3-D line geometry needs some additional criteria to fully satisfy 3-D symmetric sampling requirements. Areal geometry has its own requirements to satisfy the prescription of 3-D symmetric sampling. This extension to 3-D is discussed in the following sections.

Areal geometries

In areal geometry, the basic subsets are either 3-D common-shot gathers acquired with widely spaced shots or 3-D common-receiver gathers recorded with widely spaced receivers. Alias-free sampling of 3-D common-shot gathers requires that receivers be sampled at the basic sampling interval in x as well as in y.

On land, the basic sampling interval is usually so small that sampling at that interval becomes prohibitively expensive. An alternative to this very fine sampling is to use coarser receiver-station intervals, where alias protection is provided by areal geophone arrays. But this would mean that the whole survey area still has to be covered with geophones. A practical alternative to plastering the area with areal geophone arrays might be the use of an areal shot array (with the same dimensions as would be required for the areal geophone arrays). Even though the effect of a shot array is not identical to that of areal geophone arrays, it might come close. Another alternative is to use deep shot holes so that hardly any ground roll is generated, leading to a larger basic sampling interval. But even then, the areal geometry is very labor-intensive, making it much more expensive than an equally satisfactory orthogonal geometry.

For deep-water acquisition, the basic sampling interval is equal to the basic signal sampling interval. In that environment, areal arrays are not needed to suppress unwanted coherent energy. Moreover, covering the survey area with closely spaced shots need not be prohibitively expensive, so that the recording of 3-D common-receiver gathers using a square grid of widely spaced stationary receivers might be affordable.

Line geometries

Alias-free sampling of the 3-D subsets of line geometries requires sampling of shots and receivers along their respective acquisition lines using the basic sampling interval. Again, arrays can be used as anti-alias filters and resampling operators to allow sampling at the basic signal sampling interval. Linear arrays along the acquisition lines are sufficient to take care of the problem of aliasing noise with low apparent velocities. However, if needed, noise suppression can be improved by using areal shot and/or receiver arrays.

Parallel geometry.—In parallel geometry, it is not sufficient for the midpoint line to be sampled without aliasing, the distance between the midpoint lines also has to be considered. If that distance is small enough, the COA gathers can also be sampled alias-free in both spatial dimensions. Repeated acquisition, at small intervals, of 2-D lines produces the ideal parallel geometry (for each midpoint line, its shot-line and its receiver line coincide with it; cf. Figure 3). In case of center-spread acquisition, the COA gather is properly sampled straightaway. In marine acquisition with end-on shooting and equal shot and receiver intervals, the odd/even signal pattern (checkerboarding) in the midpoints can be remedied by de-aliasing of the common-offset gathers (by interpolation in the common-shot and the common-receiver gathers; Vermeer, 1990).

Another—quite hypothetical—way of acquiring properly sampled COA gathers is to have a constant (nonzero) cross-line offset between the source track and the receiver line. Moving this arrangement for the next midpoint line over a small distance (half the basic sampling interval) also leads to well-sampled COA gathers. In this setup, each COA gather would have its own shot/receiver azimuth.

In marine streamer acquisition, parallel geometry is more or less the rule. Unfortunately, with this, 3-D symmetric sampling is far from the rule. The first marine 3-D surveys were often shot as a series of 2-D lines, which often satisfied the 2-D symmetric sampling criteria, but which used too large line spacings, consequently requiring later reshoots. Modern streamer acquisition uses multisource multistreamer configurations. Though common–in-line-offset gathers can be extracted from such surveys, the cross-line offset varies between midpoint lines. These geometries lead to irregular subsurface illumination, even if the surface sampling is regular (Beasley and Mobley, 1995; Beasley, 1996).

The potential irregularity of subsurface sampling is illustrated in Figure 10, which shows the "footprints" of various multisource multistreamer configurations for a plane dipping layer in a constant-velocity medium. Each footprint consists of the x,y-coordinates of the reflection points for 24 adjacent midpoints in a cross-line of the geometry. Each vertical or near-vertical line in Figure 10 connects the coordinates of the reflection points corresponding to one midpoint. The reflection points corresponding to the same long offset are connected by a horizontal or near-horizontal line. The shape of the reflection point trajectories can be understood if one realizes that the reflection point moves updip, that is, toward the source when shooting downdip (sailing updip) and away from the source when shooting updip. Note that the cross-line shift of the reflection points is largest for the long offsets, even though the azimuth variation is smallest for the long offsets.

In these multisource multistreamer geometries, the shortest offsets sample the subsurface in a regular way, but the longer offsets sample the subsurface irregularly, the irregularity increasing with the range of cross-line offsets. The irregularity also depends on the in-line dip: the larger this dip, the more irregularly will the reflector be illuminated. Only the single-source single-streamer geometry samples the subsurface in a regular way.

Another reason why properly sampled subsets are not obtained in streamer acquisition is differential feathering between successive midpoint lines or boat passes. This causes even more variation of azimuth in the 3-D common-offset gathers. Figure 11 shows footprints of the same geometries as Figure 10, but now including random feathering between boat passes and assuming constant feather within a boat pass. In this case, even the single/single geometry fails to illuminate the subsurface in a regular way.

It may be noted that feathering turns the midpoint line into a midpoint area that has basically single-fold coverage. Owing to differential feathering, however, these midpoint areas

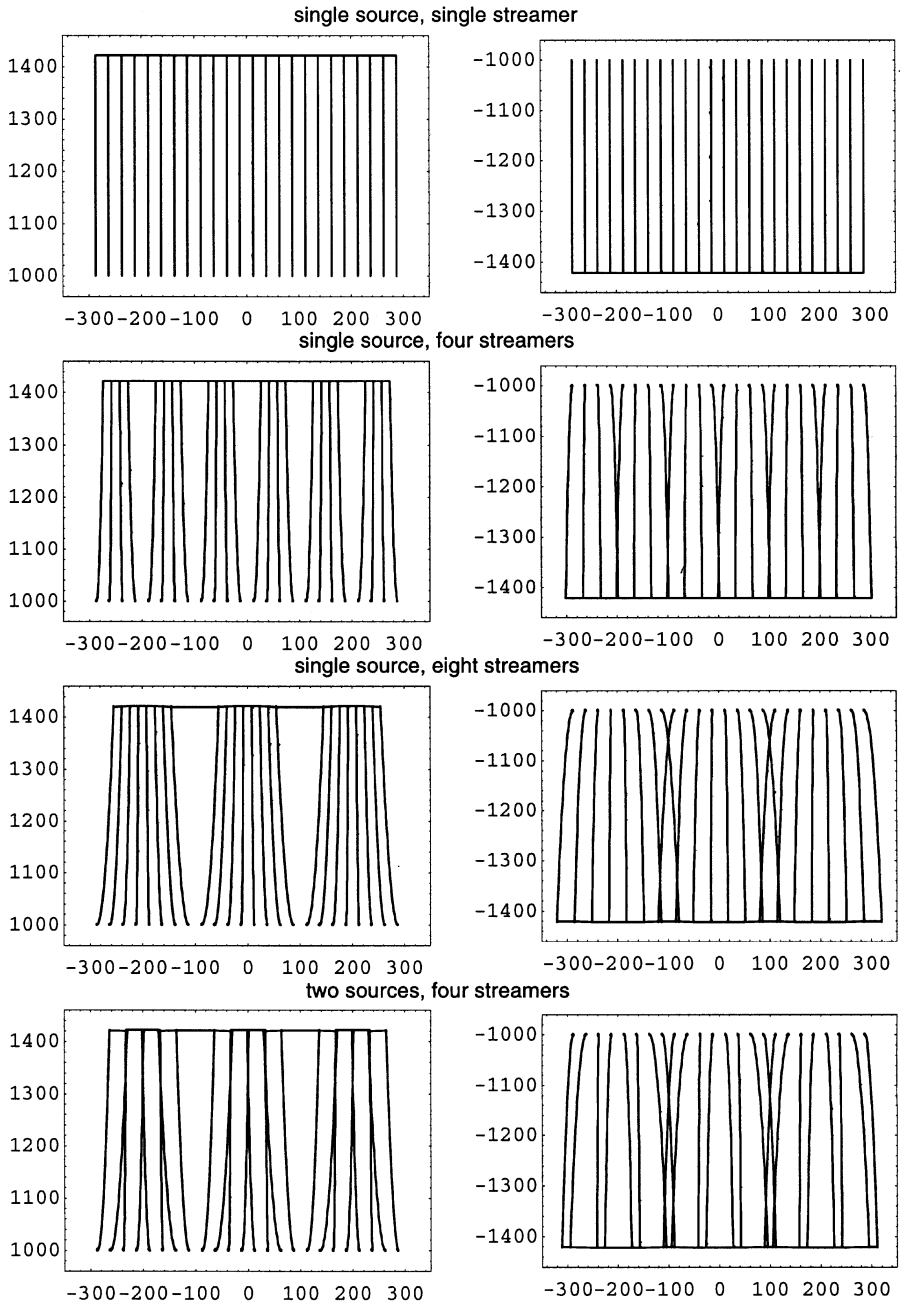

FIG. 10. Nominal footprints of multisource multistreamer configurations in the case of downdip shooting (left column) and updip shooting (right column). Each vertical or near-vertical line connects the (x, y)-coordinates of the reflection points as seen by one of 24 adjacent midpoints in the crossline direction. In every case, a reflector with 30° dip is illuminated in a constant-velocity medium. The horizontal or near-horizontal line connects the longest offsets. Note the irregular sampling of the long offsets in the cross-line direction in all cases except for the single-source single-streamer configuration.

(single-fold subsets of the "feather" geometry) do not overlap in a regular way. Normally, the feathering is not large enough to permit prestack migration of individual midpoint areas (i.e., these midpoint areas do not qualify as minimal data sets; Padhi and Holley, 1997). Only if the feathering could be made constant across the whole survey would the single-source single-streamer geometry again be ideally suited for prestack migration. In that case, each 3-D common-offset gather would have constant azimuth.

In the in-line direction, the variation in illumination caused by both multisource multistreamer acquisition and differential feathering is far less than in the cross-line direction, leading to striping of the amplitudes seen in horizon slices. Various techniques have been proposed to correct for these irregularities (e.g., Beasley and Klotz, 1992; Gardner and Canning, 1994, Huard and Spitz, 1997), but a fully satisfactory solution seems to be impossible. Hence, in cases, where the geophysical interpretation may be influenced strongly by the geometry imprint, alternative techniques to streamer acquisition using stationary-receiver systems seem to be a better way out.

Orthogonal geometry.—Besides equal shot and receiver intervals and equal shot and receiver arrays, 3-D symmetric sampling of orthogonal geometry also requires as many receivers

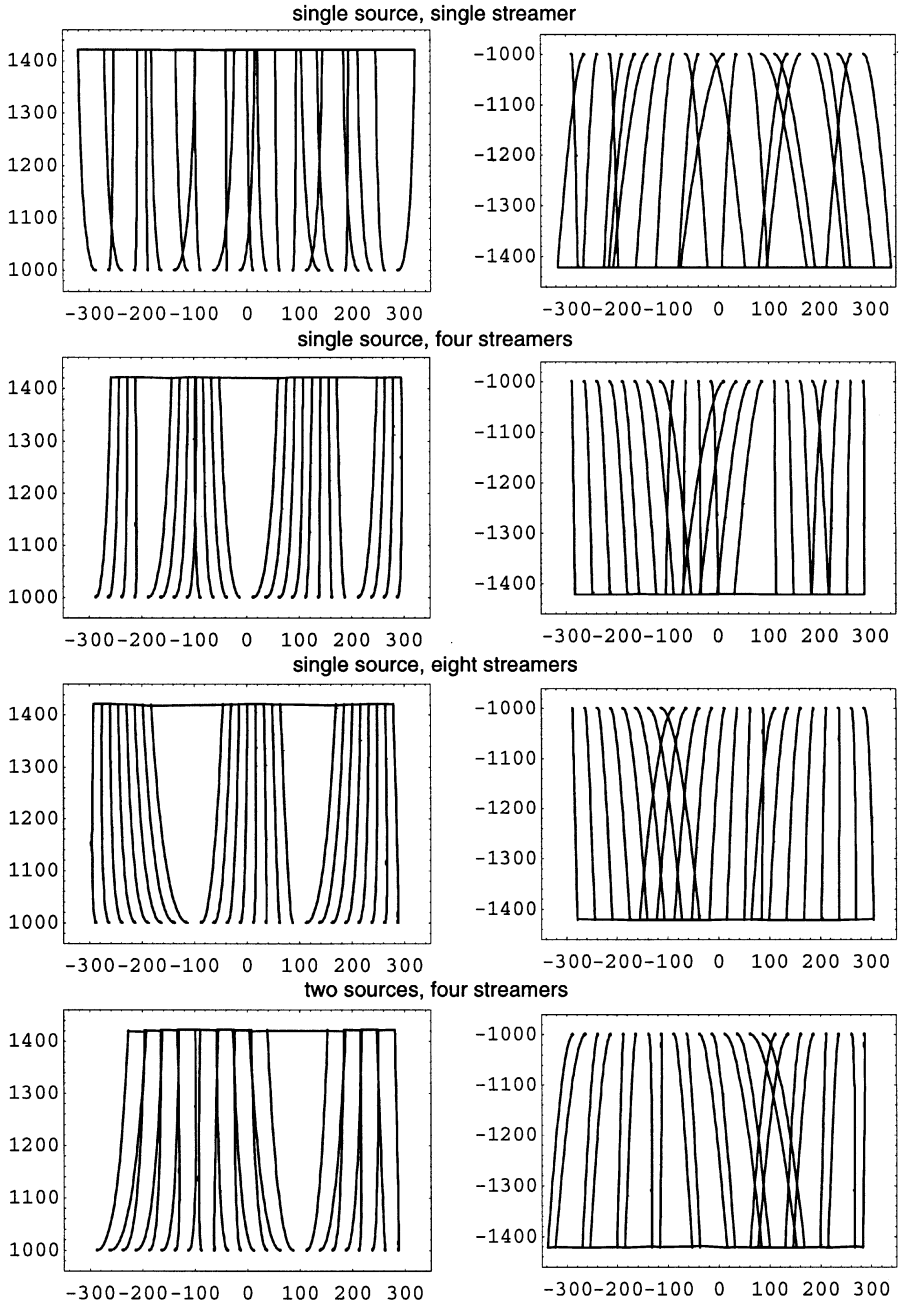

FIG. 11. Footprints of multisource multistreamer configurations with feathering. For each boat pass, a constant feathering angle was randomly selected from a uniform distribution between -2.5° and 2.5°. Otherwise, the acquisition geometries and subsurface are the same as in Figure 10. Note the dramatic departure from regularity for the single-source single-streamer geometry.

in the common shot as shots in the common receiver, and the center-spread acquisition of both shots and receivers. This recipe ensures the acquisition of square cross-spreads (the aspect ratio of the geometry equals one, as in the left side of Figure 5). The shot line interval and the receiver line interval should preferably also be the same for symmetric sampling. However, allowing some difference in shot and receiver line density in the case where shots and receivers differ in cost, would be quite acceptable in most cases.

Figure 12a shows that a linear geophone array mixes midpoints in a common-shot gather, thereby reducing the aliasing in that gather. Figure 12b shows what happens when a linear shot array (along the shot line) is introduced as well: it reduces aliasing in the common-receiver gather. Together, the linear shot and receiver arrays ensure sampling of the whole cross-spread with minimal aliasing. It should be realized that shot arrays are as important as geophone arrays; as geophone arrays will not prevent aliasing in the common-receiver gather, they are fully complementary (see also Smith, 1997).

In addition to serving as anti-alias filters and resampling operators, arrays also serve to suppress noise, such as ground roll. The first arrival of the ground roll has the shape of a cone centered on the center of the cross-spread. A common-shot cross-section through this cone has the shape of a hyperbola. The ground roll near the apex of the hyperbola will not be suppressed by the receiver arrays. This flat part of the hyperbola is centered around the shot line. The common-receiver gathers, however, cut the same part of the ground-roll cone at much larger angles. Hence, in that area, the shot arrays will suppress the ground roll. The same reasoning can be applied with shots and receivers interchanged. In other words, in the cross-spread, shot and receiver arrays are fully complementary with respect to ground-roll suppression. In those places where the shot array is less effective in suppressing ground-roll energy, the receiver array is at its best, and vice versa. If the noise is very strong, noise suppression may be improved by using areal rather than linear arrays.

In areas where shots are particularly expensive, areal receiver arrays may be considered in combination with single shots. At least for first-arrival ground roll in a homogeneous medium, the action of an N-element shot array convolved with an M-element receiver array is identical to the action of an $N \times M$-element receiver array convolved with a single shot (apart from shot strength effects). For noise traveling in other directions—back-scattered noise and side-scattered noise—the response would be different. Theoretically, an areal receiver array would not protect as much against aliasing in the common-receiver gather as would the combination of a linear shot array and a linear receiver array. As far as noise suppression is concerned, however, the areal array has a small advantage: it will always suppress energy with slow apparent velocity, irrespective of the traveling direction of the energy. Therefore, if an areal geophone array is cheaper than the combination of linear shot and receiver arrays, such a departure from symmetric sampling might be the best option.

The case for center-spread acquisition and equal maximum cross-line offset and maximum in-line offset is supported strongly by the timeslices of a square cross-spread shown in Figure 13. In the top timeslices in Figure 13, the traveltime contours are circular, corresponding to reflections from horizontal layering, whereas in the bottom timeslices in Figure 13, the traveltime contours are elliptical, corresponding to plane-dipping reflectors. Note the similarity of these latter contours to those for the cross-spread in Figure 4b. If the maximum cross-line offset were much smaller than the maximum in-line offset, the spatial continuity of the cross-spread would not be fully exploited. Figure 13 also illustrates the need for equal shot and receiver intervals; the wavefield clearly behaves in the same way in both spatial directions. Doubling the shot interval would cause aliasing in the common-receiver gathers and, hence, largely hamper the usefulness of k or f-k filters in that domain.

Even though cross-spreads have limited extent, it is possible to create single-fold coverage across the whole survey by a tiling of adjacent cross-spreads. In such a single-fold gather, the data would be piecewise continuous with discontinuities between the adjacent cross-spreads. Figure 14 shows the illumination by four adjacent cross-spreads of a reflector with 15° dip and a reflector with 45° dip. Each cross-spread covers the reflector with its own "blanket." Around the edges of these blankets gaps and overlaps exist. Within each blanket, illumination can be considered as continuous (provided the cross-spread

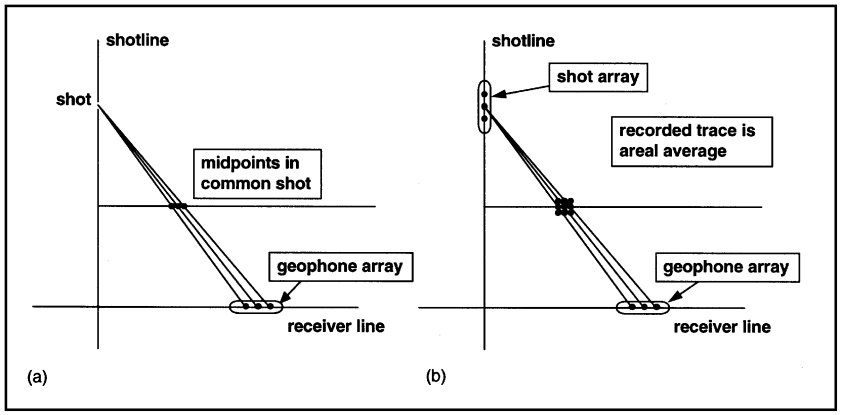

FIG. 12. Anti-aliasing by geophone array, alone (a) and in combination with shot array (b). A geophone array reduces aliasing in a common-shot gather, whereas a shot array reduces aliasing in a common-receiver gather. Together, they take care of reduced aliasing in the cross-spread. To avoid clutter, only three of the nine contributing shot/receiver segments have been drawn in (b).

is sampled alias free), but illumination is discontinuous across the edge of each blanket (see also the Appendix).

Zigzag geometry.—Alias-free sampling of the zig- and zag-spreads would require that the spacing of the traces in the common-receiver gather be the same as the trace spacing in the common-shot gather. Similarly to other geometries, this requirement would mean equal shot and receiver intervals, the shot interval being measured along the shot line.

As mentioned before, in actual practice the shot interval is the receiver interval times the square root of two. This means that alias-free sampling of the common-receiver gathers would require oversampling of the common-shot gathers. The zig- and zag-spreads (cf. Figure 9) have a constant number

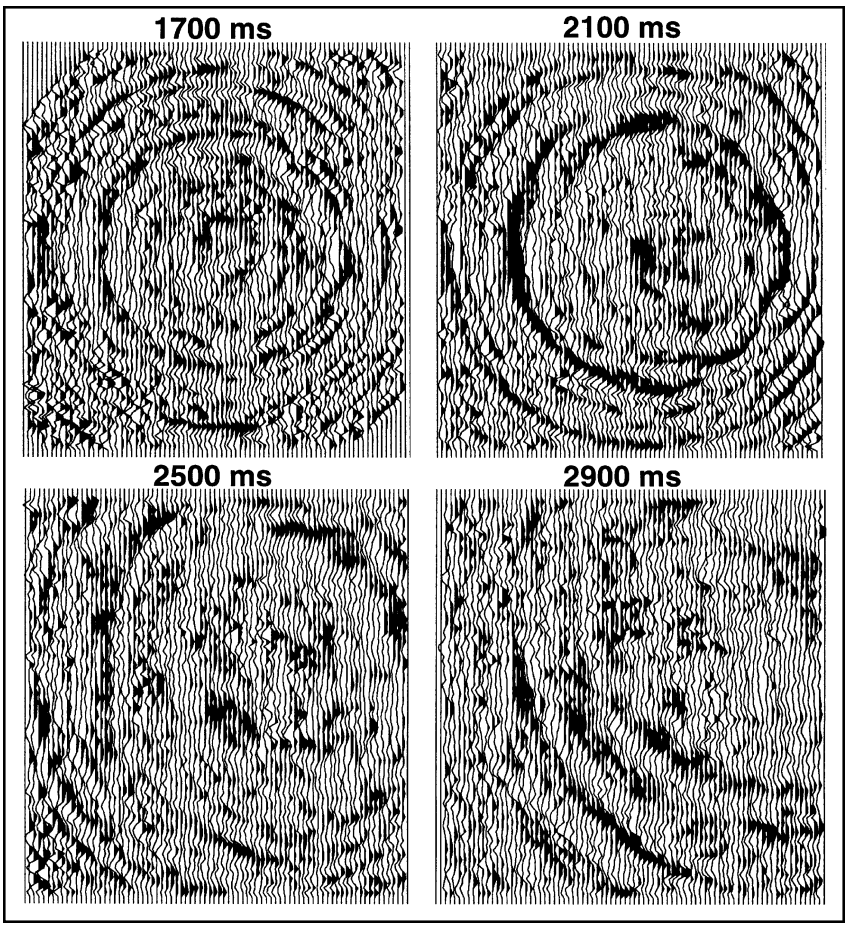

FIG. 13. Timeslices through a square cross-spread.

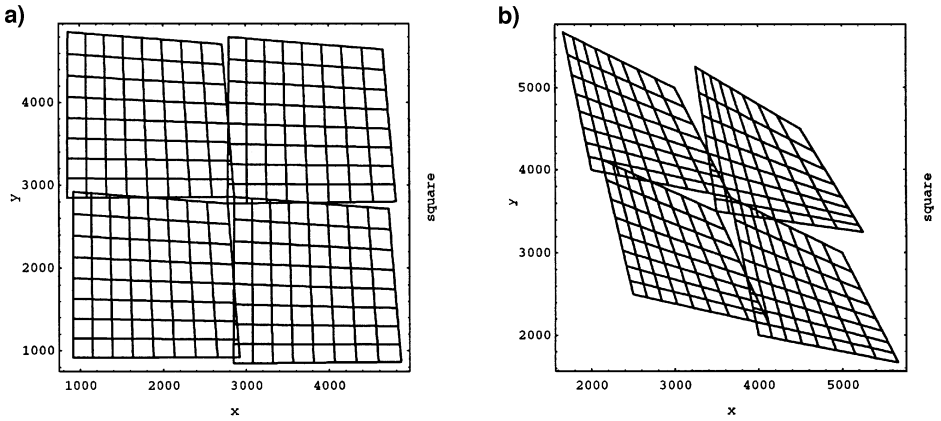

FIG. 14. Illumination of 15° (a) and 45° (b) dipping events by four adjacent cross-spreads. Note that illumination fold can be considered a continuous function inside the cross-spreads, whereas it is discontinuous across the edges of the cross-spreads.

of traces N in the common–in-line-offset gather, whereas the number of traces in the common-receiver gathers varies from one to N.

The maximum useful extent of the zig-spread is reached if the offset ellipse of the maximum useful offset touches the edges of the zig-spread as shown in Figure 9. In that case, the maximum cross-line offset equals the maximum in-line offset.

Zigzag geometry is particularly efficient in a desert environment surveyed with vibrators. The distance to be traveled by the vibrators is a factor square root of two shorter than in an equivalent orthogonal geometry, and it is much easier to avoid driving over geophones, because no sharp turns have to be made. On the other hand, it is more difficult to benefit from the spatial continuity of the subsets in prestack processing.

3-D SURVEY DESIGN ON THE BASIS OF ORTHOGONAL GEOMETRY

Orthogonal geometry is the geometry of choice for much of the land data acquisition, but it is also used in marine data acquisition in combination with ocean bottom cables. If 3-D symmetric sampling is taken as a starting point, the choice of parameters for this geometry is simplified considerably. Instead of having to decide on the shot interval and on the receiver interval, a decision need only be made as to *the* sampling interval. Similarly, the maximum in-line and maximum cross-line offsets can be made equal. It is also recommended to see what the consequences are of making the shot line interval and the receiver line interval the same. Another benefit of symmetric sampling is that the designer does not need to worry about the offset distribution: 3-D symmetric sampling automatically leads to a reasonable offset distribution.

The choice of the various parameters depends on the geophysical requirements, which in turn are often a compromise between what the interpreter would like to see and what the budget will permit. In my view, the most important geophysical requirements are: spatial continuity, resolution, shallowest horizon to be mapped, deepest horizon to be mapped, and the signal-to-noise ratio.

Spatial continuity is best served by 3-D symmetric sampling in which the single-fold cross-spreads have maximal (useful) extent, thus minimizing the number of edges and edge effects.

Resolution is determined by the maximum frequency, the velocity model, and the measurement configuration (Beylkin et al., 1985, Vermeer, 1997). As sampling can be regarded as a means of representing the integrands in the migration formulas, the quality of migration and hence the achievable resolution depends also on the sampling interval. Proper sampling of the integrands is tantamount to requiring alias-free sampling of the desired wavefield. This leads to a station spacing following from the equation

$$\Delta s = \Delta r = V_{min}/2\, f_{max}, \tag{4}$$

in which Δs and Δr are the station spacings, V_{min} is minimum apparent velocity of the recorded wavefield, and f_{max} is maximum frequency. In other words, Δs and Δr should be equal to the basic signal sampling interval needed for alias-free sampling of the desired wavefield by the cross-spread.

The *deepest horizon to be mapped* determines the maximum useful offset X_{max} to be gleaned from a mute function representative of the survey area. Often, however, the mute function of existing data ends at some shallow level because of too limited an offset range.

An important attribute in 3-D survey design is the *l*argest *m*inimum *o*ffset (*LMOS*). In combination with the mute function, *LMOS* determines the shallowest level with complete single-fold coverage. In the orthogonal geometry with equal shot and receiver line interval *S*, $LMOS = S\sqrt{2}$ (see Figure 15). In the corresponding brick-wall geometry with the same number of shots, *LMOS* is considerably smaller ($LMOS = S\sqrt{1.25}$). For many designers, this is one of the reasons to prefer brick over continuous orthogonal geometries (another reason is the stack response, which is discussed in "The stack response").

[The actual values of *LMOS* are usually somewhat smaller than given here because the pattern of shot positions is normally offset from the receiver line by half a shot station interval. The same holds for the pattern of receiver positions, which is offset from the shot line by half a station interval.]

The *shallowest horizon to be mapped* determines the fold at shallow levels. If four-fold coverage would be sufficient for mapping a shallow horizon and the largest useful offset at this level would be X_{sh}, then the largest minimum offset *LMOS* would be $X_{sh}/2$. The optimum line spacing *S* follows from $S = LMOS/\sqrt{2}$.

The line spacing is a crucial parameter: it has a great influence on the cost of the survey. Therefore, asking what is the shallowest horizon that must be mapped is perhaps a more relevant question than asking what is the shallowest level where at least single-fold coverage should exist, which is the level where the maximum useful offset is *LMOS*. Often, however, it will be difficult or downright impossible to indicate the level of the shallowest horizon to be mapped, particularly if there is no such thing as a "shallowest" horizon (e.g., when steep horizons extend all the way to the surface).

If shots are much more expensive than receivers, it should be acceptable to increase the shot line spacing while keeping *LMOS* the same by decreasing the receiver line spacing. There is a limit, of course; the shot line spacing should not be larger than the *LMOS* required for mapping the shallowest horizon.

Line spacing and maximum offset lead to a fold-of-coverage (multiplicity) M according to $M = (X_{max}/S)^2$ (or the equivalent if in-line and cross-line parameters are not the same; replace X_{max} by spread length divided by two for asymmetric shot or receiver spreads). This coverage will often be more

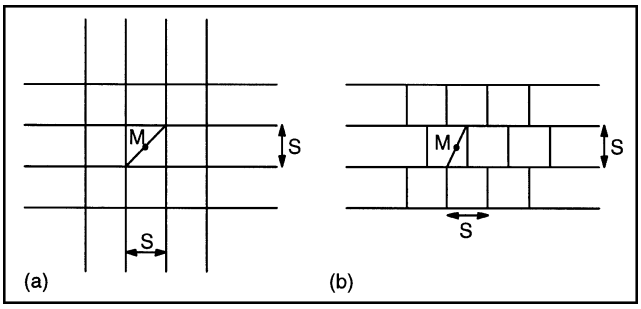

FIG. 15. Largest minimum offset *LMOS*: (a) continuous shot line geometry, (b) brick wall geometry. The minimum offset for midpoint M equals the length of the diagonal lines. The minimum offsets for other midpoints will be smaller.

than enough to achieve adequate S/N, since the maximum fold-of-coverage is already determined as soon as the required fold at shallow levels has been decided. If M is not large enough for adequate S/N, the line spacing can be decreased or areal arrays could be considered.

Noise suppression also depends on the offset distribution, which determines the stack response. For low-fold data, designers of a 3-D survey do not have to worry about the offset distribution if they adhere to 3-D symmetric sampling. The corresponding wide geometry leads automatically to an irregular offset distribution, providing the best stack response for low-fold data (see also "The stack response").

A choice for 3-D symmetric sampling has significant consequences for the distribution of offsets over the offset range. This is illustrated in Figure 16, which compares the offset distributions for a narrow and a wide (symmetric) geometry. For the same full-fold coverage, the narrow geometry builds up fold faster than the wide geometry (Figure 16a). Up to the maximum cross-line offset, the offset density builds up linearly as a function of offset. Hence long offsets dominate in wide geometry (Figure 16b).

The faster buildup of fold in the narrow geometry is a clear advantage of this geometry. But a wide geometry makes more efficient use of the shots than does a narrow geometry, so that—for the same cost—a higher maximum fold can be obtained. Additionally, the preponderance of long offsets in wide geometry gives greater weight to the long offsets than to the short offsets, leading to better suppression of multiples with a small differential moveout (cf., "Weighted stacking for multiple suppression" in Vermeer, 1990).

IMPLEMENTATION IN THE FIELD

The objective of spatial continuity and the concept of continuous fold profoundly influence the way a 3-D survey design is implemented in the field. Current practice is to aim for a regular fold as counted in bins. This regularity is achieved most easily by locating shots and receivers as close as possible to the nominal grid point position. If a shot cannot be located at that point, the standard prescription is to move the shot station over an integer number of station intervals to the right or to the left, and to move the receiver spread over an equal number of stations in the opposite direction. This prescription maintains fold and it maintains midpoints in bin centers, but it produces spatial discontinuities in the common-receiver gathers or common-shot gathers.

For optimal spatial continuity, there should be no abrupt changes in the shot and receiver positions. Each shot and receiver gather should contain a smooth subset of the 5-D prestack wavefield. Rather than jagged acquisition lines, sinuous acquisition lines should be laid out in much the same way as proposed in Lindsey (1991) for the crooked 2-D line. Moreover, sinuous lines have less impact on the environment, because they can wind around large trees (Williams, 1993). Solitary shots or receivers should always be avoided, of course.

In case an obstacle cannot be avoided by skirting around it, one may consider increasing the sampling density (along the acquisition lines) toward the obstacle, thus improving the chances for a successful interpolation across the obstacle.

SUBSET-ORIENTED PROCESSING

The stack response of low-fold data will never be very good, making it all the more important that prestack processing be carried out successfully. A major advantage of acquiring well-sampled subsets of the acquisition geometry is the possibility of applying various prestack processes on a subset-by-subset basis.

In areas where first breaks are difficult to pick, areal picking on subset-sorted data will improve the chances of making consistent picks. Dual-domain f-k filtering in cross-spreads can be even more successful than in 2-D data where both filters operate along the same midpoint line. As with shot and receiver arrays, shot-domain f-k filters and receiver-domain f-k filters are fully complementary. Cross-spreads and 3-D receiver gathers are also suited for application of a true 3-D filter.

The basic subsets are also the best domain in which to carry out interpolation, where necessary, because only two of the four spatial coordinates change at the same time (cf. Cooper et al., 1997). If there are missing shots or receivers, the neighboring shots and receivers can be used for interpolation, provided the sampling of the subsets is not too coarse. The lack of well-sampled subsets in marine streamer acquisition makes it difficult to interpolate successfully in the cross-line direction.

It is common practice to carry out picking for residual statics computation in bins or superbins. However, more reliable picking can be carried out in the basic subsets, because each trace in a subset has similar neighbors with which the cross-correlation

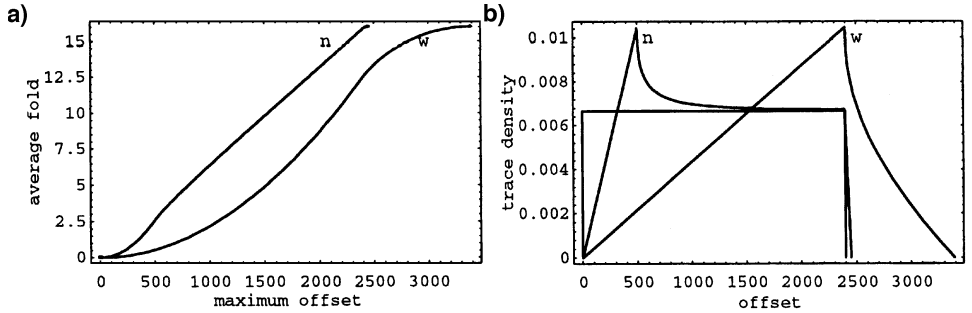

FIG. 16. Fold and trace density as functions of offset in 16-fold narrow and wide geometries. The maximum cross-line offset is 500 m for the narrow geometry ("n") and 2400 m for the wide geometry ("w"). In both cases the maximum inline offset is 2400 m. The offset distribution is considered to be a continuous function in a rectangle with the same aspect ratio as that of the geometry. For the same full-fold coverage, a narrow geometry has a faster buildup of fold than does a wide geometry. For comparison, the offset density of a parallel geometry with same full-fold coverage is shown as well in (b).

coefficient may be large. The idea of picking a grid of traces as proposed in Marcoux (1981) could be revived and adapted for this purpose.

Some geophysicists have entertained the idea that it would be best to acquire narrow swaths (cf. Figure 5) in the orthogonal geometry to make sure that the prestack data do not deviate too much from the ideal of common-offset gathers. In particular, dip moveout (DMO) would suffer from wide swaths. However, it has been shown in Vermeer et al. (1995) and in Padhi and Holley (1997) that any 3-D single-fold data set in which all traces are surrounded by near neighbors is suitable for DMO. In fact, each minimal data set is suitable not only for DMO but also for imaging the illuminated part of the subsurface by means of prestack migration. Schleicher et al. (1993) developed the conditions for true-amplitude prestack migration of minimal data sets.

THE STACK RESPONSE

For 2-D seismic data, stacking can suppress coherent noise much better than random noise if the offsets are regularly and densely sampled (Vermeer, 1990). The stack response of a CMP stack with an offset interval of dx has best suppression around wavenumber $k = 1/(2dx)$ and has aliases for $k = n/dx$, n being an integer number. In well-sampled 2-D data, the first alias of the stack response ($n = 1$) coincides with the first notch of the field arrays (though only for horizontal events). This observation regarding 2-D data has led to the widespread belief that 3-D survey design should aim for regular offset distributions.

Yet, even for 2-D data, a regular offset distribution is not ideal in general. If the fold-of-coverage is halved by doubling the shot interval, the offset sampling in the CMPs doubles, leading to a first alias of the stack response at half the original wavenumber. This is illustrated in Figure 17. Figure 17a shows the stack response of a 48-fold stack, Figure 17b the stack response of a 24-fold stack. The first alias in Figure 17b may pass a considerable amount of coherent noise, which was not suppressed by the field arrays either. For low-fold data, it is better to randomize the offset distribution, as shown in Figure 17c, since a periodicity in the offset distribution in a CMP allows the corresponding wavenumbers to escape suppression. A random offset distribution, however, suppresses coherent noise about as well as it suppresses random noise. Hence, for low-fold data, it is best to have an irregular offset distribution, that is, the CMP should show no periodicities in offset, yet cover the whole range of offsets.

In 3-D surveys, the fold-of-coverage is usually much smaller than in 2-D. If so, a regular offset distribution would produce peaks in the stack response, through which coherent noise events could pass. Selecting a wide orthogonal geometry leads automatically to an irregular offset distribution, making the stack responses of the various bins as flat as possible on average. Narrow geometries tend to produce periodicities in the offset distribution, leading to peaks in the stack response. This is illustrated in Figure 18, which shows the average stack responses of two narrow geometries and a wide geometry. Note that the stack response of the brick-wall geometry shows the same peaks as the narrow continuous geometry, except for the first peak.

Double-zigzag geometry represents a special case. For a small aspect ratio, each CMP in this high-fold geometry has a nearly regular offset distribution, leading to a very good stack response (the first strong peak in the stack response occurs at a high wavenumber due to the high fold). Figure 19 shows the stack responses of a single zigzag and a double-zigzag geometry. The single zigzag has a peak at $k = 1/400\ \mathrm{m}^{-1}$, corresponding to the period of the zigzag. In the double zigzag, this periodicity is removed by the interaction of the two zigzags. It should be realized that in a wide double-zigzag geometry the offsets are distributed less regularly, leading to a random-noise type suppression.

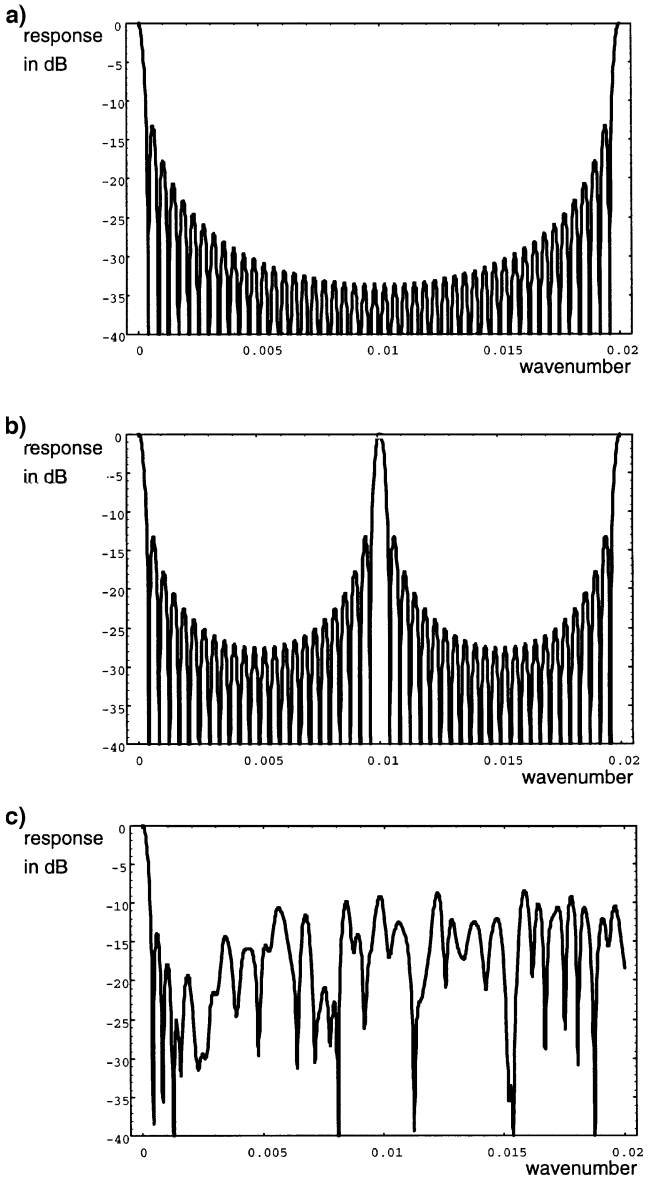

FIG. 17. Stack responses of 2-D geometries: (a) regular 48-fold, (b) regular 24-fold, and (c) irregular 24-fold. The first alias in the case of the regular 48-fold stack occurs at $k = 0.02$, where no significant coherent noise may be present. However, the first alias of the response of the 24-fold stack, which has double the trace interval of (a), may pass a significant amount of noise. The irregular 24-fold stack, which covers the same offset range as (b) suppresses coherent energy everywhere about as much as it suppresses random noise.

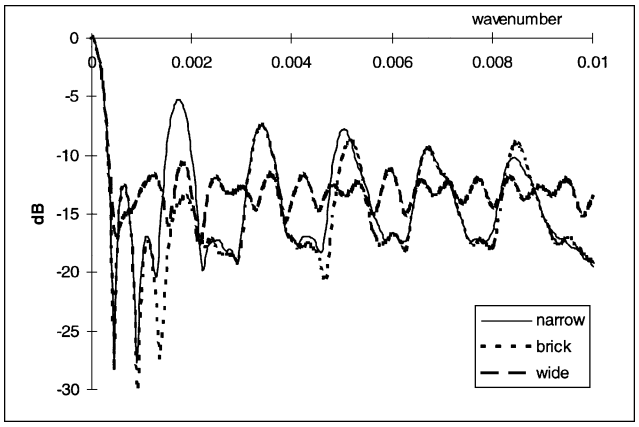

FIG. 18. Average stack responses of three 16-fold 3-D geometries. The most pronounced peaks occur in the narrow continuous geometry. The response for the brick geometry is similar to that for the narrow geometry, although it does not show a large peak close to $k = 0.002$. The wide geometry suppresses all coherent energy about as much as it suppresses random noise.

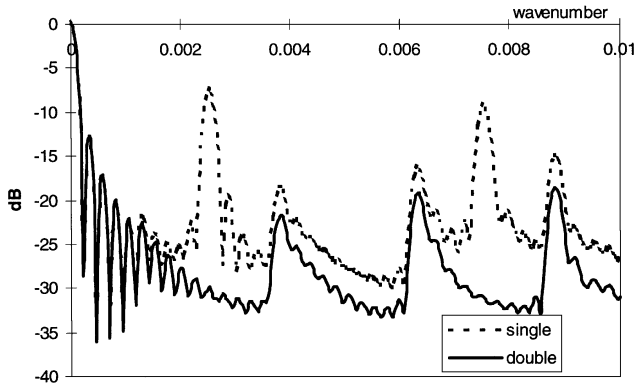

FIG. 19. Average stack responses of zigzag geometries. Shown are the stack responses for a 44-fold single zigzag geometry and an 88-fold double-zigzag geometry. In both cases, four receiver lines are spaced at 200 m, and the inline shot interval and receiver station interval are 50 m.

In a wide geometry, prestack processing can take care of the ground roll energy that is not going to be suppressed by the stack. Also migration suppresses much of the energy that does not fit the migration model (Smith and McKinley, 1996). Therefore, the not-so-good stack response of wide geometries can be compensated to some extent in processing. Only for a severe multiple problem—and in the absence of a good prestack multiple-elimination program—it may be necessary to use a narrow double-zigzag geometry for suppression of the multiples by stacking.

CONCLUSIONS

For all intents and purposes, it is impossible to properly sample the whole 5-D prestack wavefield. Three-dimensional symmetric sampling prescribes the next best alternative: the proper sampling of single-fold basic subsets of 3-D geometries. Such sampling allows optimal prestack processing, and it takes care of a design criterion that is often overlooked: spatial continuity.

If the design of 3-D surveys is based on 3-D symmetric sampling, the choice of parameters for the survey is simplified and can be approached in a systematic and scientifically sound way. Nevertheless, even with 3-D symmetric sampling as a starting point, 3-D design requires careful thought to find the best compromise between quality and cost.

The objective of spatial continuity profoundly influences the way in which practical survey problems need to be addressed. Traditionally, seismic data acquisition has concentrated on obtaining the prescribed fold. With 3-D symmetric sampling, physics, rather than statistics, is used.

ACKNOWLEDGMENTS

I thank Kees Hornman for many useful discussions and a first review of this paper. I am greatly indebted to my former Shell colleagues Raphic van der Weiden and Kees van der Kolk for their critical review and many suggestions for improvement. Numerous suggestions for improvement by the SEG reviewers, in particular Ken Larner, further improved the readability of this paper. I thank Shell International Exploration and Production B.V. for support received in preparing this paper.

REFERENCES

Anstey, N., 1986, Whatever happened to ground roll?: The Leading Edge, **5**, no. 3, 40–45.
Ball, J. D., and Mounce, W. D., 1967, Apparatus for converting lineal seismogram sections into an areally presented seismogram: U.S. Patent 3, 327, 287.
Beasley, C. J., 1996, Statistical measures of subsurface illumination: 58th Conference, Eur. Assn. Geosci. Eng., Extended Abstracts, paper B043.
Beasley, C. J., and Klotz, R., 1992, Equalization of DMO for irregular spatial sampling: 62nd Ann. Internat. Mtg., Soc. Expl. Geophys., Expanded Abstracts, 970 –973.
Beasley, C. J., and Mobley, E., 1995, Spatial sampling characteristics of wide-tow marine acquisition: 57th Conference, Eur. Assn. Geosci. Eng., Extended Abstracts, paper B031.
Becker, C. H., 1960, Method of geophysical exploration: U.S. Patent 2, 925, 138.
Berni, A. J., 1994, Remote sensing of seismic vibrations by laser Doppler interferometry: Geophysics, **59**, 1856 –1867.
Bertelli, L., Mascarin, B., and Salvador, L., 1993, Planning and field techniques for 3-D land acquisition in highly tilled and populated areas—today's results and future trends: First Break, **11**, No. 1, 23–32.
Beylkin, G., 1985, Imaging of discontinuities in the inverse scattering problem by inversion of a causal generalized Radon transform: J. Math. Phys., **26**, 99–108.
Beylkin, G., Oristaglio, M., and Miller, D., 1985, Spatial resolution of migration algorithms: *in* Berkhout, A. J., Ridder, J., and van der Waals, L. F., Eds., Proceedings of the 14th Internat. Symp. on Acoust. Imag., 155–167.
Bleistein, N., 1987, On the imaging of reflectors in the earth: Geophysics, **52**, 931–942.
Claerbout, J. F., 1985, Imaging the earth's interior: Blackwell Scientific Publ.
Cohen, J. K., Hagin, F. G., and Bleistein, N., 1986, Three-dimensional Born inversion with an arbitrary reference: Geophysics, **51**, 1552–1558.
Cooper, N. J., Williams, R. G., Wombell, R., and Notfors, C. D., 1997, An improved 3-D DMO implementation for orthogonal cross-spread acquisition geometries: EAGE Extended Abstracts, paper A051.
Crews, G. A., Henderson, G. J., Musser, J. A., and Bremner, D. L., 1989, Applications of new recording systems to 3-D survey designs: 59th Ann. Internat. Mtg., Soc. Expl. Geophys., Expanded Abstracts, 624–631.
Dickinson, J. A., Fagin, S. W., and Weisser, G. H., 1990, Comparison of 3-D seismic acquisition techniques on land: 60th Ann. Internat. Mtg., Soc. Expl. Geophys., Expanded Abstracts, 913–916.
Dunkin, J. W., and Levin, F. K., 1971, Isochrons for a three-dimensional seismic system: Geophysics, **36**, 1099–1137.
Durrani, J. A., French, W. S., and Comeaux, L. B., 1987, New directions for marine 3-D surveys: 57th Ann. Internat. Mtg., Soc. Expl. Geophys., Expanded Abstracts, 177–180.
Dürschner, H., 1984, Dreidimensionale Seismik in der Exploration auf Kohlenwasserstoff-Lagerstätten: J. Geophys., **55**, 54 –67.

Ferber, R., 1977, What is DMO coverage?: 59th Conference, Eur. Assn. Geosci. Eng., Extended Abstracts paper A049.
Gardner, G. H. F., and Canning, A., 1994, Effects of irregular sampling on 3-D prestack migration: 64th Ann. Internat. Mtg., Soc. Expl. Geophys., Expanded Abstracts, 1553–1556.
Goodway, W. N., and Ragan, B., 1997, "Mega-Bin" land 3D seismic: Toward a cost effective "symmetric patch geometry" via regular spatial sampling in acquisition design with co-operative processing, for significantly improved S/N & resolution: Proc. Soc. Expl. Geophys. Summer Research Workshop.
Huard, I., and Spitz, S., 1997, An application of 3D filtering to the restoration of missing traces: 59th Conference, Eur. Assn. Geosci. Eng., Extended Abstracts, paper A038.
Krail, P. M., 1991, Case history vertical cable 3D acquisition: 53rd Conference, Eur. Assn. Expl. Geophys., Extended Abstracts, 206.
———1993, Sub-salt acquisition with a marine vertical cable: 63rd Ann. Internat. Mtg., Soc. Expl. Geophys., Expanded Abstracts, 1376.
Lee, S. Y., Allen, K. P., Hinkley, D. L., Meek, R. A., and Laster, S. J., 1994, Pseudo-wavefield study using low fold 3-D geometry: 64th Ann. Internat. Mtg., Soc. Expl. Geophys., Expanded Abstracts, 926–929.
Lindsey, J. P., 1991, Crooked lines and taboo places: what are the rules that govern good line layout?: The Leading Edge, **10**, No. 11, 74–77.
Marcoux, M. O., 1981, On the resolution of statics, structure, and residual moveout: Geophysics, **46**, 984–993.
Moldoveanu, N., Adessi, D., Lang, J. T., Stiver, K., and Chang, M., 1994, Digiseis-enhanced streamer surveys (DESS) in obstructed area: A case study of the Gulf of Mexico: 64th Ann. Internat. Mtg., Soc. Expl. Geophys., Expanded Abstracts, 872–875.
Naylor, R., 1990, Positioning requirements for complex multi-vessel seismic acquisition: Hydrographic J., **58**, 25–32.
O'Connell, J. K., Kohli, M., and Amos, S., 1993, Bullwinkle: A unique 3-D experiment: Geophysics, **58**, 167–176.
Onderwaater, J., Wams, J., and Potters, H., 1996, Geophysics in Oman: GeoArabia, **1**, 299–324.
Ongkiehong, L., and Askin, H., 1988, Towards the universal seismic acquisition technique: First Break, **5**, 435–439.
Padhi, T., and Holley, T. K., 1997, Wide azimuths—why not?: The Leading Edge, **16**, 175–177.
Pleshkevitch, A., 1996, Cross gather data—a new subject for 3D prestack wave-equation processing: 58th Conference, Eur. Assn. Geosci. Eng., Extended Abstracts, paper 137.
Reilly, J. M., 1995, Comparison of circular "strike" and linear "dip" acquisition geometries for salt diapir imaging: The Leading Edge, **14**, 314–322.
Ritchie, W., 1991, Onshore 3-D acquisition techniques: a retrospective: 61st Ann. Internat. Mtg., Soc. Expl. Geophys., Expanded Abstracts, 750–753.
Schleicher, J., Tygel, M., and Hubral, P., 1993, 3-D true-amplitude finite-offset migration: Geophysics, **58**, 1112–1126.
Smith, J. W., 1997, Simple linear inline field arrays may save the day for 3D direct-arrival noise rejection: Proc. Soc. Expl. Geophys. Summer Research Workshop.
Smith, J. W., and McKinley, H. J., 1996, Now what's happened to ground roll? A 3D perspective on linear-moveout noise rejection: 66th Ann. Internat. Mtg., Soc. Expl. Geophys., Expanded Abstracts, 72–75.
Stone, D. G., 1994, Designing seismic surveys in two and three dimensions: Soc. Expl. Geophys.
Stubblefield, S. A., 1990, Marine walkaway vertical seismic profiling: US patent 4,958,328.
Vermeer, G. J. O., 1990, Seismic wavefield sampling: Soc. Expl. Geophys.
———1991, Symmetric sampling: The Leading Edge, **10**, No. 11, 21–27.
———1994, 3D symmetric sampling: 64th Ann. Internat. Mtg., Soc. Expl. Geophys., Expanded Abstracts, 906–909.
———1995, Discussion On: "3-D true-amplitude finite-offset migration," Schleicher, J., Tygel, H., and Hubral, P., authors: Geophysics **60**, 921–923.
———1997, Factors affecting spatial resolution: 67th Ann. Internat. Mtg., Soc. Expl. Geophys.
Vermeer, G. J. O., den Rooijen, H. P. G. M., and Douma, J., 1995, DMO in arbitrary 3D geometries: 65th Ann. Internat. Mtg., Soc. Expl. Geophys., Expanded Abstracts, 1445–1448.
Walton, G. G., 1971, Esso's 3-D seismic proves versatile: Oil and Gas J., **69**, No. 13, 139–141.
———1972, Three-dimensional seismic method: Geophysics, **37**, 417–430.
Wams, J., and Rozemond, J., 1997, Recent developments in 3-D acquisition techniques in Oman: GeoArabia, **2**, 205–216.
Williams, K., 1993, Trends in seismic data acquisition—a perspective: CSEG Recorder, **18**, No. 10, 14–16.

APPENDIX

A DISCUSSION OF "FOLD"

Fold, fold-of-coverage, and multiplicity are all expressions for the same notion. Usually, fold is thought of as the number of traces sharing the same midpoint (in 2-D acquisition) or the number of traces sharing the same bin (in 3-D acquisition). However, it is appropriate and instructive to describe fold—at any surface position—also as the number of overlapping midpoint areas of the 3-D subsets of the 5-D prestack wavefield. In other words, fold can also be considered as a continuous function of the midpoint coordinates of overlapping subsets. In the concept of continuous fold, fold is discontinuous at the edges of any subset, unless the subset is adjacent to another subset. This concept of continuous fold might be exploited to derive a measure of the spatial continuity of a geometry. Note, however, that this description of fold cannot be applied in geometries that are inherently spatially discontinuous, such as the multisource multistreamer configurations (see "Parallel geometry" within the subsection "Line geometries," and also Beasley and Mobley, 1995).

The concept of continuous fold is not new. It was already used to describe fold for 2-D data, where it is known that each receiver spread length produces single-fold coverage along a distance equal to half the spread length. If fold is counted correctly, there should be no difference between the continuous fold count and the discrete fold count. Disparities may arise if the binsize of a geometry is enlarged. In my view, it is incorrect to call the ensuing increase of number of traces in each bin an increase in fold.

The concept of continuous fold-of-coverage can be extended to continuous fold-of-illumination, image fold, and DMO fold. Each (continuous) midpoint area corresponds to a continuous area on any reflector that has been illuminated (the area of specular points corresponding to the midpoint area). Fold-of-illumination at any point is just the number of overlapping illuminated areas (see also the discussion of Figure 14). Each area that has been illuminated can be imaged, apart from incomplete images along the edges of illuminated areas. Therefore, the image fold is at best equal to the illumination fold. From each point of a single-fold area of illumination, a normal-incidence ray may be traced to the surface, giving rise to a surface area for which DMO images can be constructed. The DMO fold at any point corresponds to the number of such overlapping surface areas at that point. Because of edge effects, the DMO fold is at best equal to illumination fold. For another definition of DMO fold, see Ferber (1997).

A consequence of the concept of image fold is that in CIP (common image point) analysis the number of image traces should not be larger than the expected image fold. If it is, some of the image traces will show incomplete images, which may give rise to false analysis results.